

# An Artificial Intelligence - Powered Evaluation of Aurantiamide as Inhibitor against Multiple Sclerosis

Yamuna V\*, Guhan G<sup>1</sup>

*\*,<sup>1</sup>Department of Pharmaceutical Chemistry, College of Pharmacy, Madras Medical College ,  
Chennai-600 003, India.*

Date of Submission: 15-11-2024

Date of Acceptance: 25-11-2024

## ABSTRACT:

Multiple Sclerosis (MS) is a complex and multifactorial disease characterized by chronic inflammation, demyelination, and neurodegeneration in the central nervous system (CNS). Computer-aided drug design has gained popularity and proven to be a useful tool for cutting down on time and resources, especially in the early stages of the drug development and discovery process. The right enzyme target is found using the SuperPred 3.0 platform. The SwissADME and the Osiris property explorer are used for In-silico ADMET evaluation. Protein repair and analysis server (PRAS) is used to prepare proteins that were retrieved from the RCSB databank. The webserver

CB-DOCK2 is used for active site prediction and docking. The Biovia Discovery Studio is used to visualise docking results. The Cabsflex 2.0 and the fastDRH server are used for Molecular dynamics and re-scoring computations, respectively. According to the current study, Aurantiamide is a non-toxic, orally accessible ligand that can effectively inhibit certain receptors/enzymes in the field of drug discovery. Aurantiamide may therefore be regarded as a lead in the development of medications. We also realised that the drug discovery process is accelerated by AI-guided drug design.

**KEYWORDS:** Multiple Sclerosis, Neprilysin, Cathepsin D, CADD.

## I. INTRODUCTION

Multiple sclerosis (MS) is a chronic autoimmune disease that primarily affects the central nervous system (CNS), which includes the brain, spinal cord, and optic nerves. In MS, the immune system mistakenly attacks the protective covering of nerve fibers known as myelin, leading to inflammation and damage. This demyelination disrupts the transmission of electrical signals between the brain and the rest of the body, resulting in a variety of neurological symptoms[1].

The term "Computer-Aided Drug Design," or "CADD," is commonly used to refer to the systematic and rational development of new medicines through the application of computational techniques and methodologies. CADD has gained popularity and proven to be a tremendous time and resource saver, especially in the early stages of the drug discovery and development pipeline[2]. Several popular CADD methods include Molecular docking, Molecular dynamic modelling, Scaffold hopping, Pharmacophore mapping, similarity search, and Quantitative Structure-Activity Relationship (QSAR)[3].

Aurantiamide can be extracted from a number of plants, including *Portulaca oleracea* L, *Clematis terniflora* DC, *Gomphrena celosioides* etc with number of biological activities including anti-

oxidant, anti-platelet, anti-inflammatory, and anti-tumor[4-6]. The present study also aims to evaluate the Aurantiamide as inhibitor against Multiple sclerosis through the In-silico approach.

## II. MATERIALS AND METHODS TARGET FISHING AND DATA CURATION

To identify the best target for screening, the Superpred 3.0 platform is utilised (<https://prediction.charite.de/>) [7]. For the screening procedure, the structure of the Aurantiamide was obtained in the structure data file (SDF) format from the PubChem database (<https://pubchem.ncbi.nlm.nih.gov/>)

## ADMET PREDICTION

The most crucial factor in determining how a drug works is its ADMET properties. The drug-likeness profiling based on adsorption, distribution, metabolism, and excretion is carried out in the current study using the SWISSADME (<http://www.swissadme.ch/index.php>)[8]. The SWISSADME was used to input the SMILES notation that was taken from the Pubchem database. The compound's toxic effects are predicted using Osiris Property Explorer (<https://openmolecules.org/>)

## DOCKING STUDIES

### PROTEIN RETRIEVAL AND PREPARATION

The RCSB protein data bank was used to obtain the 3D structures of Neprilysin (PDB CODE: 6SUK) and Cathepsin D (PDB CODE: 4OD9). After that, it is entered into the Protein Repair and Analysis Server (PRAS- <https://www.protein-science.com/>) to check for and fix any missing hydrogen atoms, heavy atoms, or residues [9]. The PROCHECK suite of programs (<https://saves.mbi.ucla.edu/>) analyses the overall structure geometry and residue-by-residue geometry to check the stereochemical quality of a imported protein structure [10]. The ERRANT webserver (<https://saves.mbi.ucla.edu/>) used to determine protein quality by plotting the value of the error function against the location of a 9-residue sliding window, which is determined by comparing the statistics from highly refined structures with the statistics of non-bonded interactions between various atom types [11]. The VERIFY3D program (<https://saves.mbi.ucla.edu/>) assigns a structural class based on the location and environment of an atomic model (3D) (alpha, beta, loop, polar, nonpolar, etc.) and compares the results to good structures to determine whether the model is compatible with its own amino acid sequence (1D) [12]. 2D and 3D Ramachandran plots of various types was generated using RAMPLOT (<https://ramplot.in/index.php>) to aid in the analysis of protein structures

### LIGAND PREPARATION

The MM2 force field tool of the Chem3D module in the ChemBioOffice software package is used to subject the ligand to the energy minimisation step.

### BINDING CAVITY PREDICTION

The CB-DOCK2 webserver is used to predict the binding cavity. It clusters the solvent accessible surface and uses a structure-based method to predict cavities. It provides important details about the volume, size, and centre of the anticipated cavities. (<https://cadd.labshare.cn/cb-dock2/index.php>) [13].

### DOCKING AND VISUALIZATION STUDY

The Autodock vina module of the CB-DOCK2 webserver is used for docking, and the

Biovia Discovery Studio software 2021 is used to visualise the binding interactions.

### MOLECULAR DYNAMICS (MD) SIMULATION

The protein is simulated using the Cabs Flex 2.0 webserver. Greater flexibility is indicated by a maximum RMSF value, whereas the system was constrained during the simulation run by a minimum value. (<https://biocomp.chem.uw.edu.pl/CABSflex2>) [14]

### MOLECULAR MECHANICS – GENERALIZED BORN SURFACE AREA SOLVATION (MM-GBSA) CALCULATION

A web server called fastDRH has been made available to the public for free in order to predict and analyse the structures of protein–ligand interactions. This server's user-friendly and adaptable web platform effectively integrated different poses-based per-residue energy decomposition analysis and structure-truncated MM/PB(GB)SA free energy calculation processes. It comprises the docking protocol based on the AutoDock Vina and AutoDock-GPU docking engines that the user specifies. The overview can be found at (<http://cadd.zju.edu.cn/fastdrh/overview>) [15]

### CHARACTERIZATION NMR AND MASS SPECTROSCOPY

The 1D NMR and 2D NMR (COSY and HECTOR) spectrum of the compound Aurantiamide was analyzed using NMRium software, (<https://www.nmrium.org/>) [16] while the mass spectrum was also determined utilizing CFMID from WishartLab at the energies 10V, 20V, 40V by the input the SMILES notation that was taken from the Pubchem database. (<https://cfmid.wishartlab.com/>) [17]

## III. RESULTS AND DISCUSSION TARGET FISHING

The target, Cathepsin D with a 98.95% model accuracy and an 96.88% probability score and Neprilysin with a 92.63% model accuracy and an 60.16% probability score was predicted by SuperPred software. Multiple sclerosis is the indication of the anticipated target. Figures No. 1 and No.2 show the outcomes of the predicted targets and indications.

Target Name	ChEMBL-ID	UniProt ID	PDB Visualization	TTD ID	Probability	Model accuracy
Protein Mdm4	CHEMBL1255126	O15151	6Q9Y	T36741	97.73%	90.2%
Cyclooxygenase-1	CHEMBL221	P23219	6Y3C	Not Available	97.64%	90.17%
Cathepsin D	CHEMBL2581	P07339	4OD9	T67102	96.88%	98.95%
Bloom syndrome protein	CHEMBL1293237	P54132	4O3M	Not Available	96.48%	70.06%
Neprilysin	CHEMBL1944	P08473	6SUK	T05409	60.16%	92.63%
Histone deacetylase 5	CHEMBL2563	Q9UQL6	5UWI	Not Available	59.79%	89.67%

Fig.No.1: Predicted targets for the Aurantiamide using SuperPred server

Target Name	ChEMBL-ID	Indication	Probability	Model accuracy
Protein Mdm4	T36741	Acute myeloid leukaemia [ICD-11: 2A60]	97.73%	90.2%
Protein Mdm4	T36741	Haematological malignancy [ICD-11: 2B33.Y]	97.73%	90.2%
Protein Mdm4	T36741	Myelodysplastic syndrome [ICD-11: 2A37]	97.73%	90.2%
Protein Mdm4	T36741	Solid tumour/cancer [ICD-11: 2A00-2F9Z]	97.73%	90.2%
Cathepsin D	T67102	Hypertension [ICD-11: BA00-BA04]	96.88%	98.95%
Cathepsin D	T67102	Multiple sclerosis [ICD-11: 8A40]	96.88%	98.95%
Cathepsin L	T41141	Abdominal aortic aneurysm [ICD-11: BD50.4]	93.92%	96.61%
Neprilysin	T05409	leukaemia [ICD-11: 2A60-2B33]	60.16%	92.63%
Neprilysin	T05409	Multiple sclerosis [ICD-11: 8A40]	60.16%	92.63%
Neprilysin	T05409	Non-small-cell lung cancer [ICD-11: 2C25.Y]	60.16%	92.63%

Fig. No.2 : Predicted indications for the Aurantiamide using SuperPred server

## ADMET RESULTS

Aurantiamide exhibits good GI absorption and complies with the Lipinski rule. Cytochrome enzyme CYP1A2 are not inhibited by it. It has bioavailability score of 0.55. When drug likeness filters like Lipinski, Ghose, Egan, and Muegge are followed, it is clear that Aurantiamide has the potential to be a safe oral medication. The synthetic accessibility score, which ranges from 0 to 10, it lies at 3.27, indicating that it is easily synthesised. The presence of BBB permeation is necessary for its

efficient operation. The Table No. 1 displays the ADMET findings derived from the Osiris property explorer and SWISSADME. For toxic endpoints like mutagenicity, tumorigenicity, irritation, and reproductive toxicity, Osiris Property Explorer has determined that the compound "Aurantiamide" is non-toxic. As a result, Aurantiamide may be used safely in medicine. Furthermore, a drug-score of 0.64 indicates that the compound is a lead molecule that fights Multiple sclerosis. The Aurantiamide ADMET results are displayed in figures 3 and 4.

Table.No.1: ADMET results using the SWISSADME and Osiris property explorer

COMPOUND	M.W (g/mol)	LOGP	TPSA (Å)	GI ABSORPTION	LIPINSKI RULE	TOXICITY
Aurantiamide	402.49	2.95	78.43	High	Obey	No

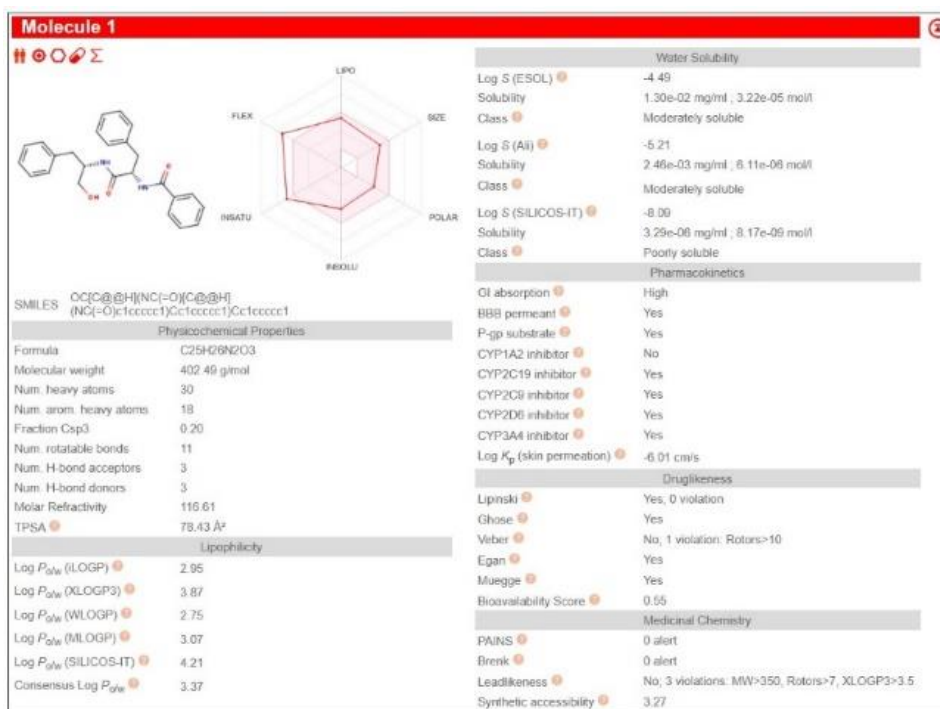


Fig. No.3: SwissADME results for the Aurantiamide

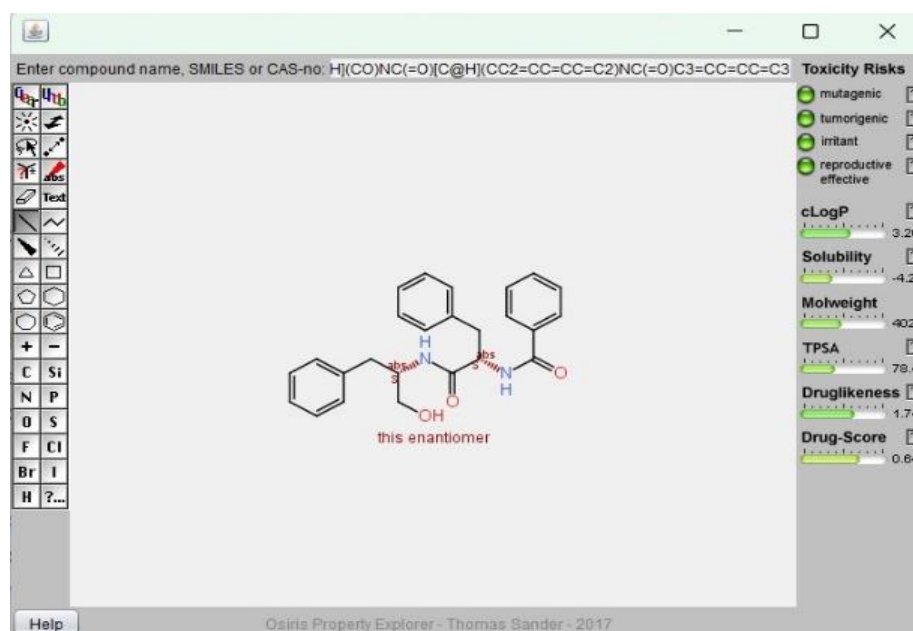


Fig. No.4: Toxicity profile of Aurantiamide by the OSIRIS software

## DOCKING RESULTS

The protein was repaired and secondary structure information of the targets are also

determined using the PRAS server that are given below in the fig.no.5

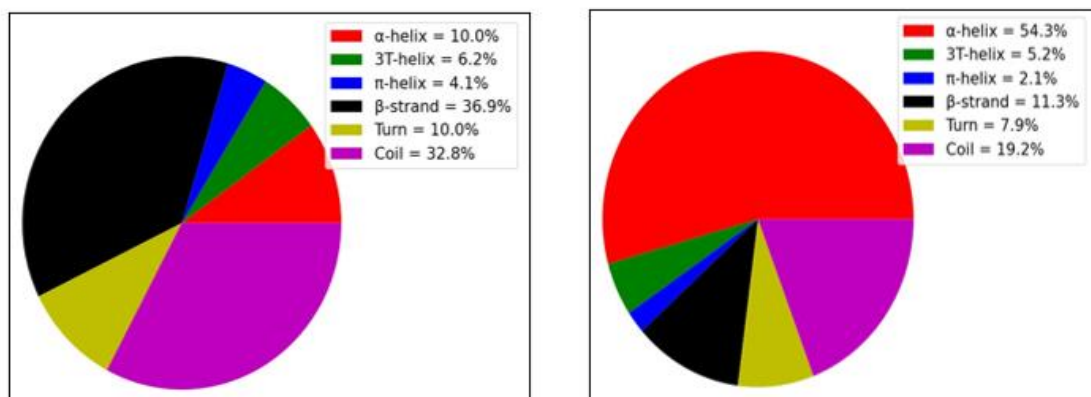


Fig. No. 5: Secondary Structure information for target- Cathepsin D and Neprilysin

The PROCHECK software tool is used to validate the protein structure. The protein is then used in additional docking studies after more than 90% of the amino acid residues are located in the most advantageous area of the Ramachandran plot. The Ramachandran plot for the Protein Id: 4OD9 and 6SUK is shown in the fig.no.6. It is found that 92.5% residues lie in the most favored region, 7.5%

residues in the additional allowed region for Protein Id 4OD9 and 93.4% residues lie in the most favored region, 6.5% residues in the additional allowed region for Protein Id 6SUK. The 2D and 3D Ramachandran plots of various types was also generated using RAMPLOT for the analysis of protein structures which are given in figures below as 7, 8, 9, 10 and 11

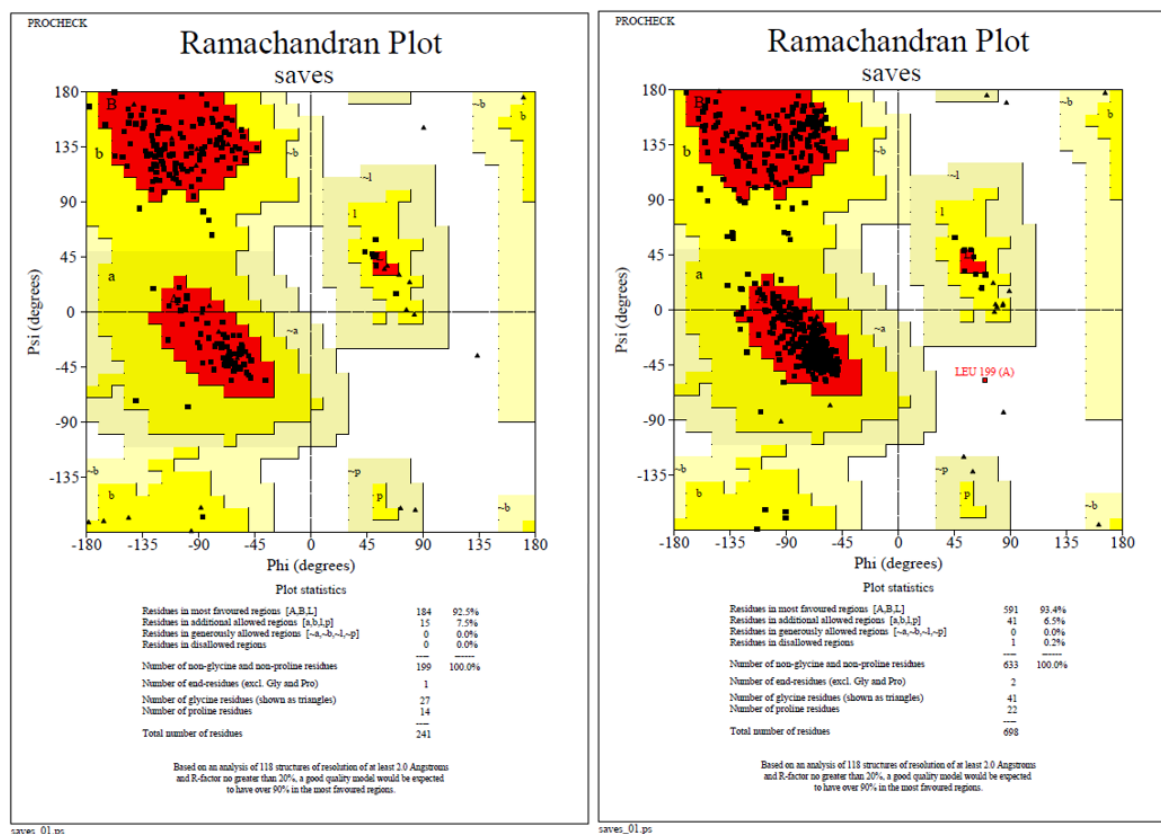
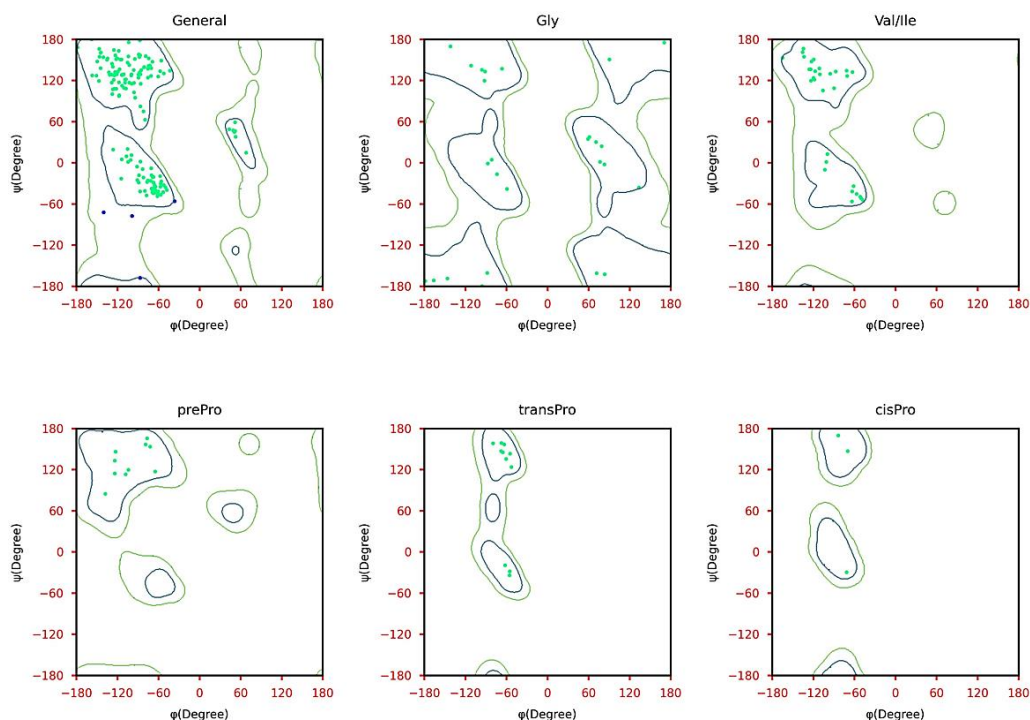
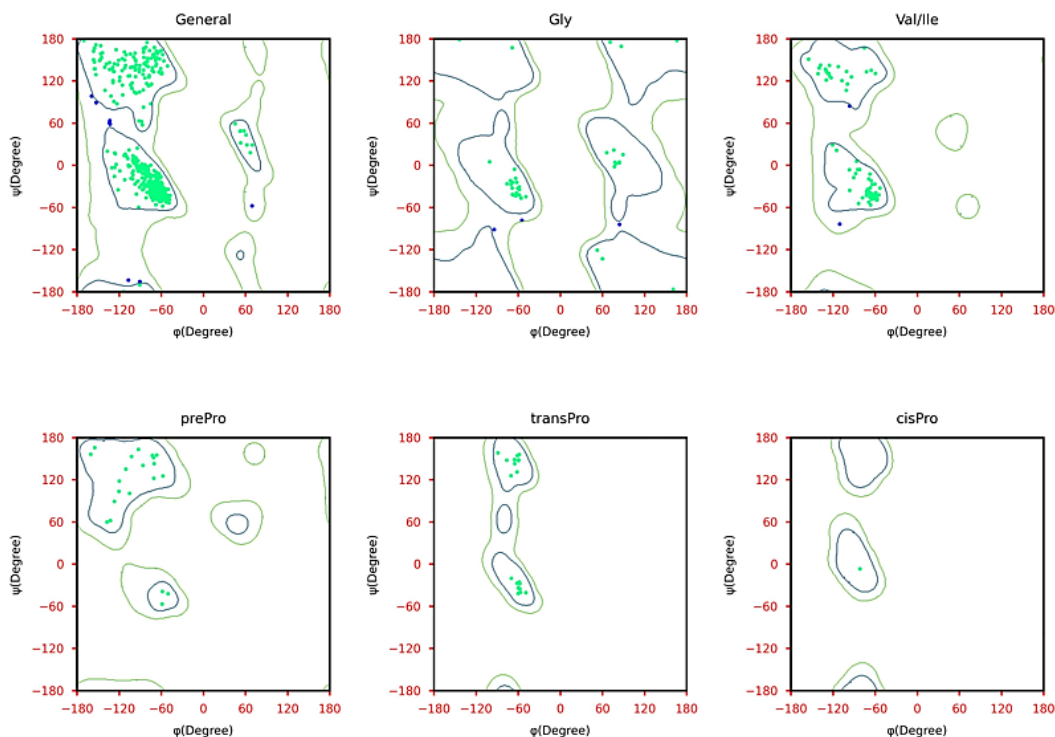


Fig. No.6: Ramachandran plot for the PDB ID: 4OD9 and PDB ID: 6SUK





**Fig. No. 7: 2D Ramachandran plot of six distinct categories plot for the PDB ID: 4OD9**



**Fig. No. 8: 2D Ramachandran plot of six distinct categories plot for the PDB ID: 6SUK**

The six distinct categories are general case (Ala and remaining 15 amino acids), Gly,Val/Ile, pre-Pro, trans-Pro & cis-Pro. Here, green blue and

red dots represent torsion angles of favoured, allowed and disallowed regions respectively.

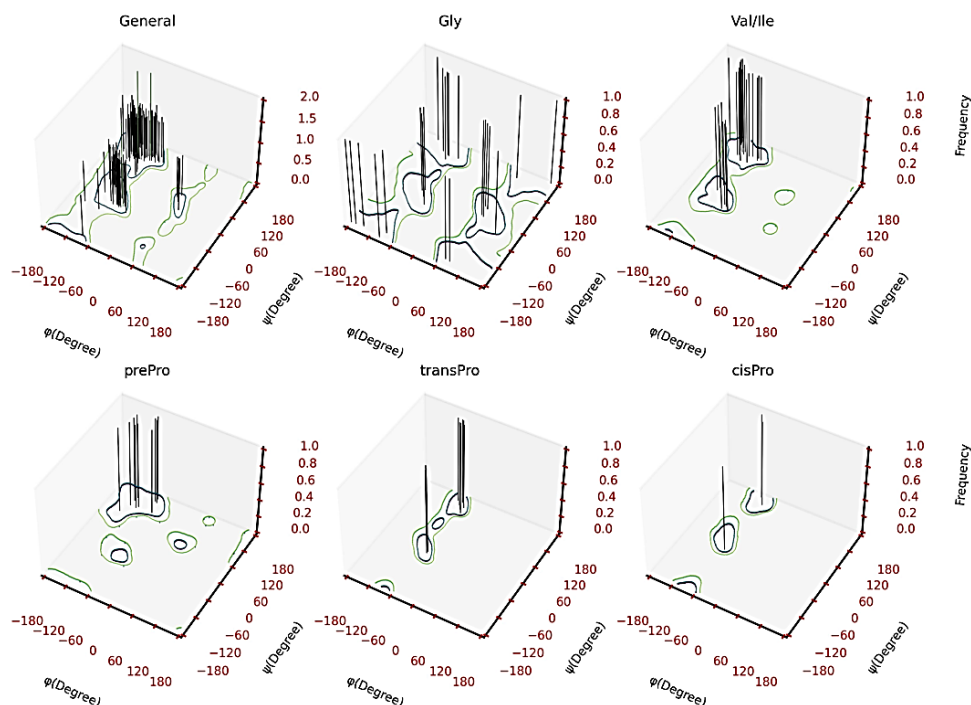


Fig. No.9: 3D Ramachandran plot of six distinct categories plot for the PDB ID: 4OD9

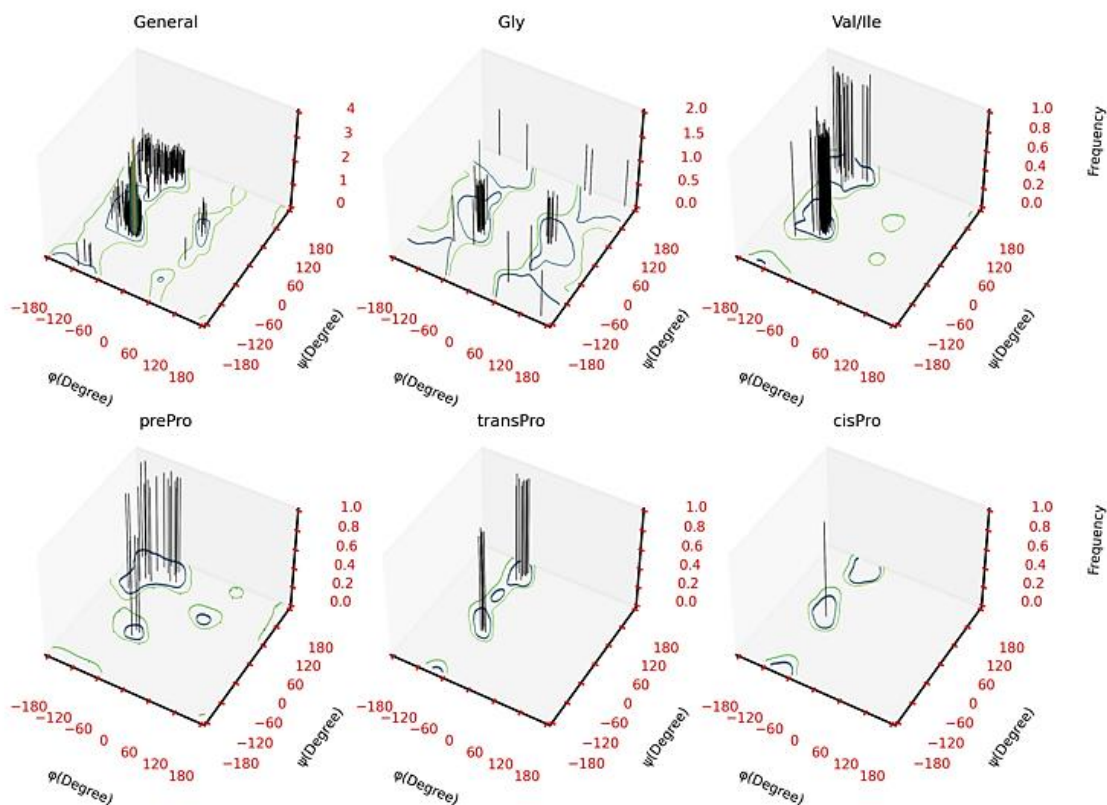
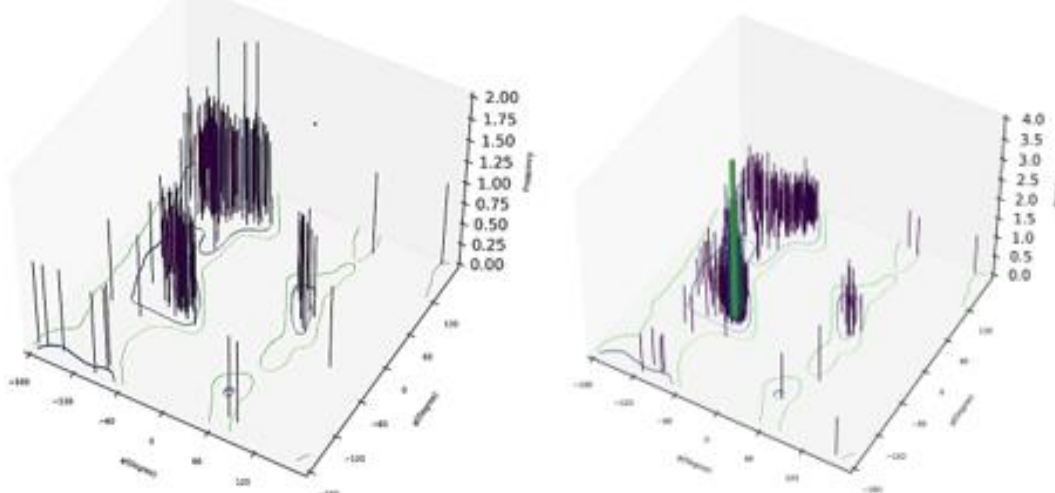


Fig. No.10: 3D Ramachandran plot of six distinct categories plot for the PDB ID: 6SUK

The six distinct categories are general case (Ala and remaining 15 amino acids), Gly, Val/Ile, pre-Pro,

trans-Pro & cis-Pro. Here, bars represent frequency of torsion angles



**Fig. No.11: Standard 3D Ramachandran plot for the PDB ID: 4OD9 and 6SUK**

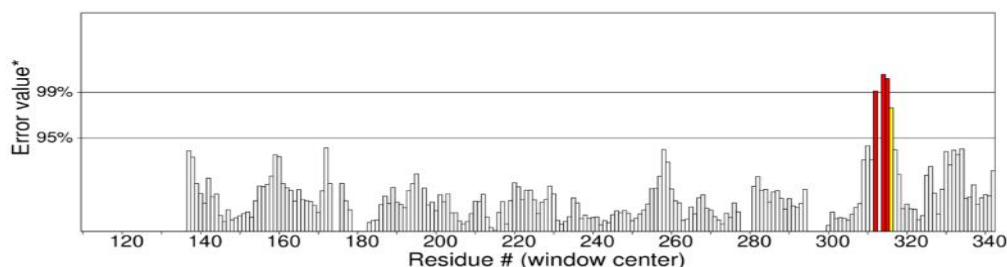
Here, bar represents frequency of torsion angles.

The value of the error function against the location of a 9-residue sliding window was plotted for the proteins to evaluate the quality of protein structure using Errat Webserver. The overall quality factor of Protein ID: 4OD9 was 97.895 and the overall quality factor of Protein ID: 6SUK was 98.986. They are represented in figure. No 12 and 13

The compatibility of the protein's 3D structure with its amino acid sequence was

evaluated by using VERIFY3D program. For Protein ID 4OD9, 74.69% of the residues have averaged 3D-1D score  $\geq 0.1$  and fewer than 80% of the amino acids have scored  $\geq 0.1$  in the 3D/1D profile. For Protein ID 6SUK, 88.40% of the residues have averaged 3D-1D  $\geq 0.1$  and at least 80% of the amino acid have scored  $\geq 0.1$  in the 3D/1D profile. The graphical representation of the proteins are given as figure no 14 and 15.

Program: ERRAT2  
File: 4OD9.pdb  
Chain#:D  
Overall quality factor\*\*: 97.895

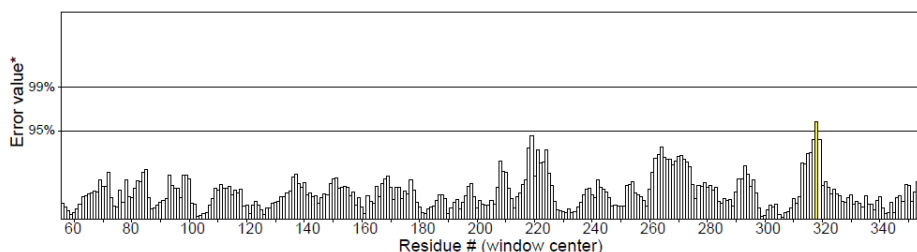


\*On the error axis, two lines are drawn to indicate the confidence with which it is possible to reject regions that exceed that error value.  
\*\*Expressed as the percentage of the protein for which the calculated error value falls below the 95% rejection limit. Good high resolution structures generally produce values around 95% or higher. For lower resolutions (2.5 to 3Å) the average overall quality factor is around 91%.

**Fig. No.12 : Errat plot for PDB ID: 4OD9**



Program: ERRAT2  
File: protein2.pdb  
Chain#:A  
Overall quality factor\*\*: 98.986



\*On the error axis, two lines are drawn to indicate the confidence with which it is possible to reject regions that exceed that error value.  
\*\*Expressed as the percentage of the protein for which the calculated error value falls below the 95% rejection limit. Good high resolution structures generally produce values around 95% or higher. For lower resolutions (2.5 to 3Å) the average overall quality factor is around 91%.

Fig. No. 13 : Errat plot for PDB ID: 6SUK

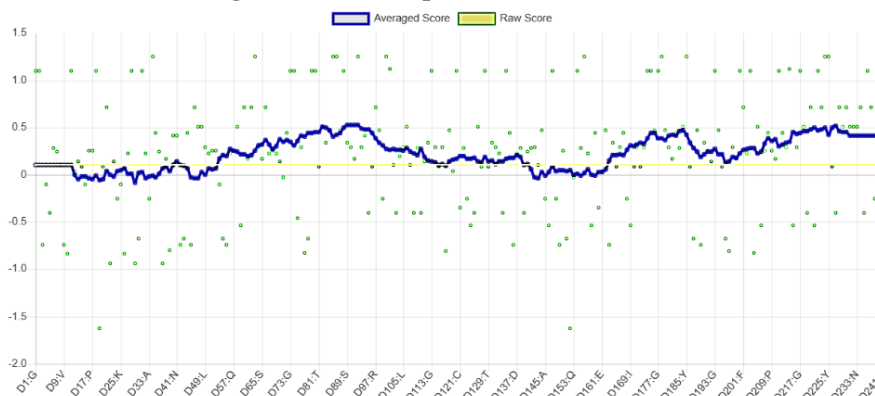


Fig. No. 14 : VERIFY 3D structure for PDB ID: 4OD9

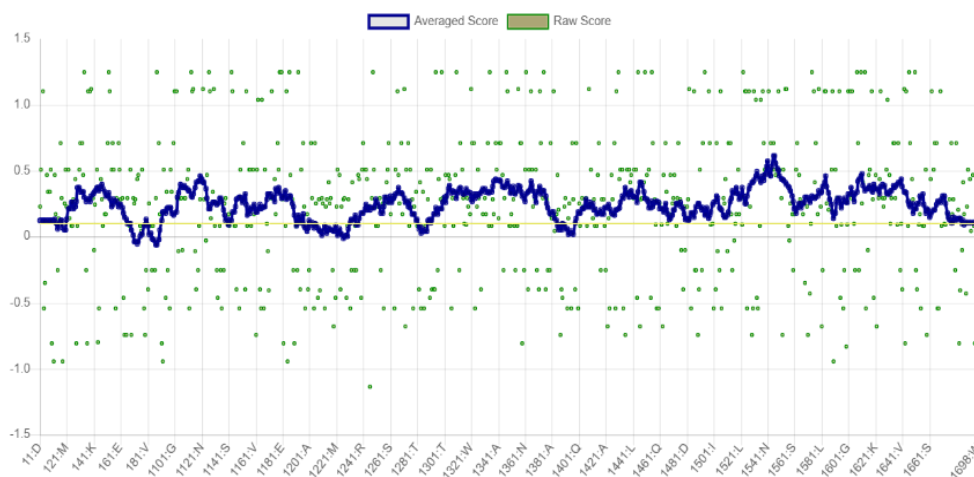


Fig. No.15: VERIFY 3D structure for PDB ID: 6SUK

The table no.2 shows the details about the binding cavity volume, size, and docking scores that was obtained by CB-DOCK2 webserver

Table . No. 2 : Docking Attributes Result

Docking Attributes	Protein	
	Cathepsin D	Neprilysin
Docking score	-8.2 kcal/mol	-9.3 kcal/mol
Binding cavity details	Cavity volume :152 Å <sup>3</sup>	Cavity volume : 2108 Å <sup>3</sup>
	Center (x,y,z) :-20, -7, -11	Center (x,y,z) : 10, -44, 3
	Cavity size :24, 24, 24	Cavity size : 24, 24, 34

From the docking study, Aurantiamide forms a stable complex with docking score of -8.2 kcal/mol and -9.3 kcal/mol. The figure.no.16, 17, 18, 19 represents the docking pose, interactions etc.

Notably, the Aurantiamide forms essential hydrogen bonding, electrostatic, and Vander-Waals interactions.

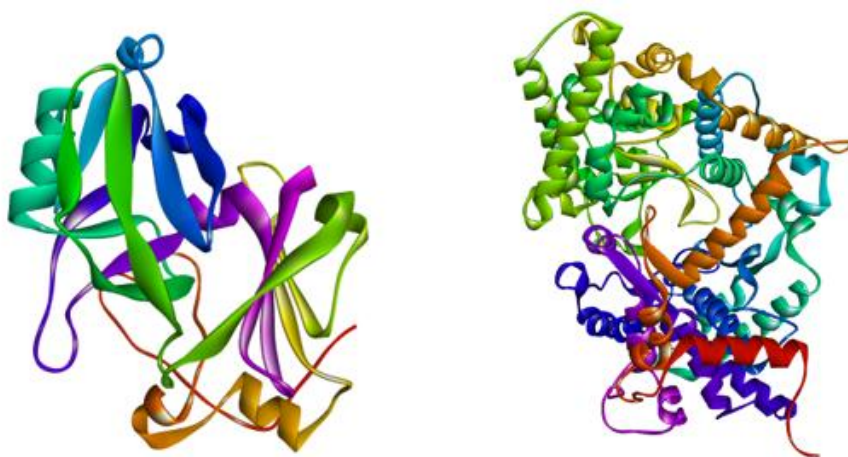


Fig. No.16: 3D structure of Cathepsin D and Neprilysin against Aurantiamide

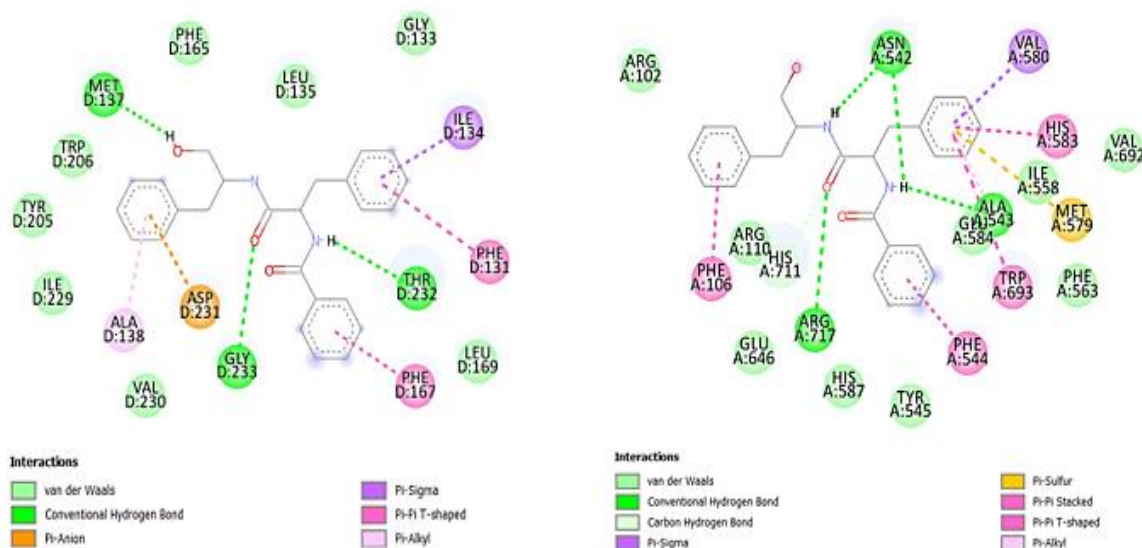


Fig. No.17 : Binding interaction of Cathepsin D - Aurantiamide complex and Neprilysin - Aurantiamide complex

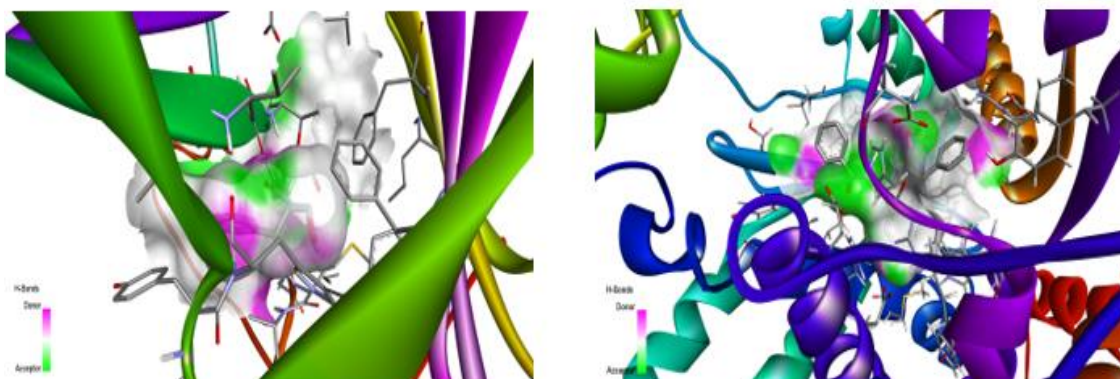


Fig. No.18 : Hydrogen bond surface of Cathepsin D and Neprilysin

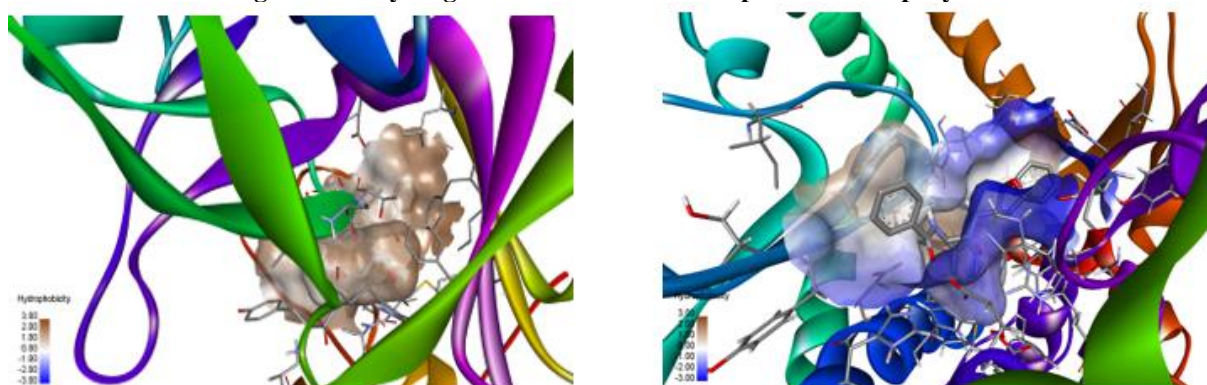


Fig. No.19 : Hydrophobic surface of Cathepsin D and Neprilysin cavity with Aurantiamide complex.

## MOLECULAR DYNAMICS (MD) SIMULATION

The protein and the protein-ligand complex are subjected to MD simulation in the Cabs flex 2.0 webserver. With a global weight of 1.0 and a temperature of 1.4, 50 cycles and trajectory frames were chosen. When their RMSF (root mean square fluctuation) values are compared, a notable drop in

the fluctuation's levels suggests that the protein-ligand complex is stable. The fact that every protein residue exhibits fluctuations below the 4 angstroms is noteworthy. The fig.no.20 represents the RMSF plot of Cathepsin D and Neprilysin. The fig.no.21 represents the RMSF plot of Cathepsin D - Aurantiamide and Neprilysin- Aurantiamide complex.

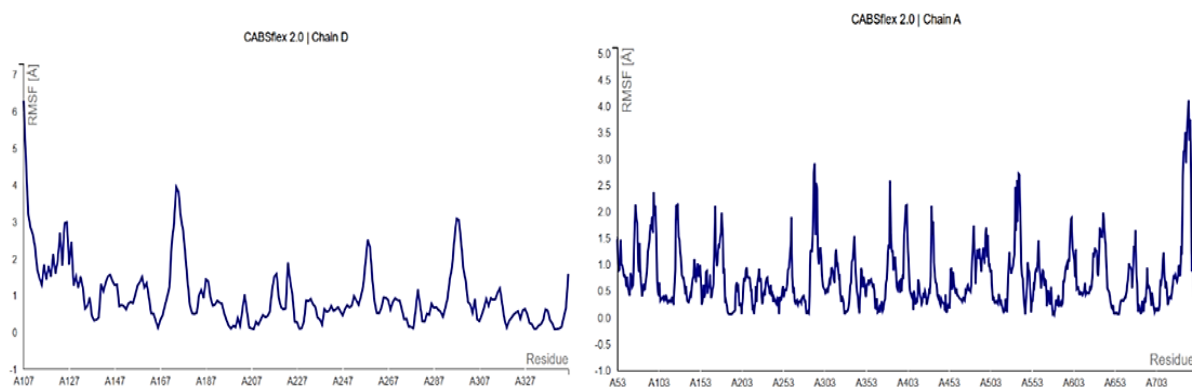


Fig. No. 20 : RMSF plot of Cathepsin D and Neprilysin

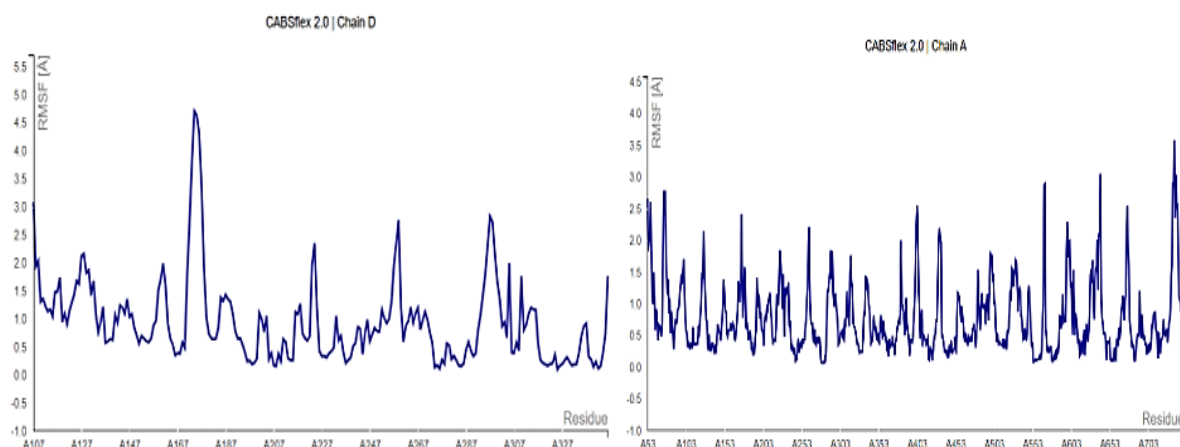


Fig. No. 21 : RMSF plot of the Cathepsin D - Aurantiamide and Neprilysin- Aurantiamide complex.

### MM-GBSA ANALYSIS

The complex's stability is demonstrated by the binding affinity of -26.38 kcal/mol, which is displayed by the MM-GBSA calculations performed in the FastDRH server. The table lists the MM-

GBSA scores for each of the Aurantiamide's different poses. According to the results of hotspot residue analysis (Perresidue decomposition) the best pose interacts with the amino-acid residues which are shown in figures 22 and 23

Table. No.3 : MM-GBSA calculations for different protein

POSE	MM GBSA SCORE	POSE	MM GBSA SCORE
pose001	-35.94	pose001	-33.76
pose002	-28.51	pose002	-27.42
pose003	-31.55	pose003	-34.19
pose004	-32.67	pose004	-27.73
pose005	-28.04	pose005	-29.6
pose006	-28.48	pose006	-23.01
pose007	-32.74	pose007	-28.01
pose008	-29.62	pose008	-31.45
pose009	-30.57	pose009	-27.78
pose010	-30.12	pose010	-24.86

For Protein

Cathepsin D

For Protein

Neprilysin

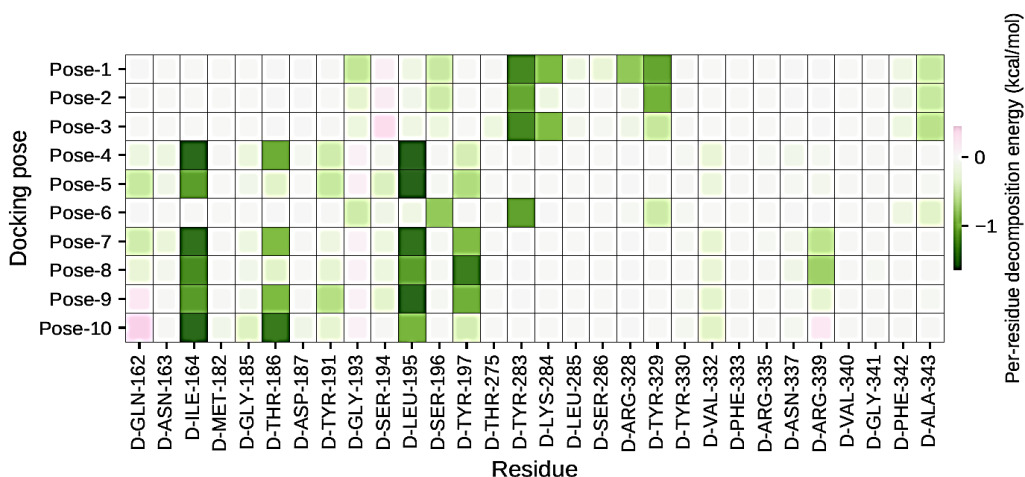


Fig. No. 22 : Hotspot residues predicted by using the FastDRH server for Cathepsin D



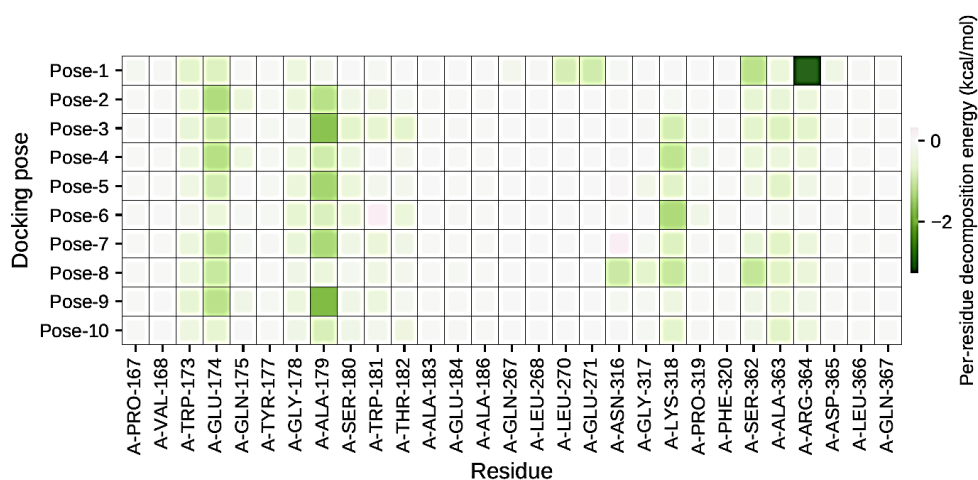


Fig. No. 23 : Hotspot residues predicted by using the FastDRH server for Neprilysin

### MASS SPECTROSCOPY

SMILES notation that was taken from the Pubchem database of the compound were inputted in the CFMID webserver and the spectra type was set to ESI with Ion mode-Positive then the mass

spectrum was generated for the compound - Aurantiamide at the different energies of 10V, 20V, 40V. Input parameters for spectrum prediction was given below

Parent Compound Structure (SMILES Format)	C1=CC=C(C=C1)C[C@@H](CO)NC(=O)[C@H](CC2=CC=CC=C2)NC(=O)C3=CC=CC=C3
Parent Compound Mass	402.1943427021
Spectra Type	ESI
Ion Mode	Positive
Adduct Type	[M+H] <sup>+</sup>
Probability Threshold	0.001
Status	Completed

Fig. No. 24 : Input parameters for spectrum prediction

### Predicted spectra are shown below

Peaks for which corresponding fragments have been found are colored red; unassigned peaks are colored blue. However select over the peaks to see the exact mass and intensity values, along with

the highest scoring assigned fragments, if found. By Clicking on red spectra lines will show a list of all possible predicted fragments for that peak. A list of all possible matching fragments is shown below the spectra.

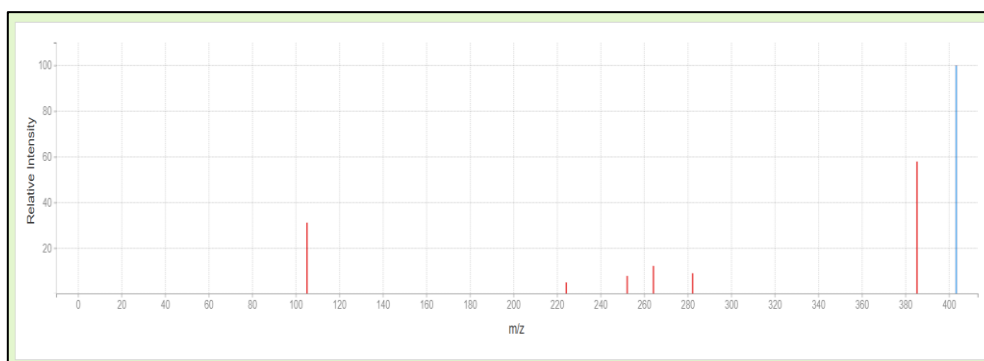


Fig. No.25 : Predicted Low Energy MsMs Spectrum (10V), [M+H]<sup>+</sup>



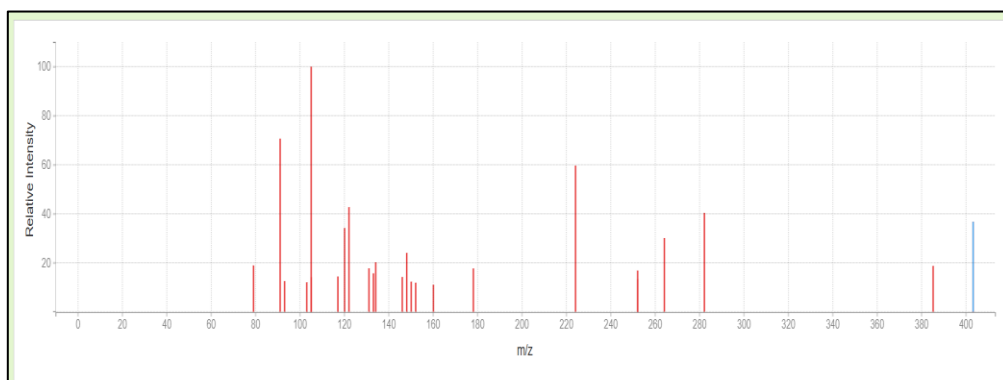


Fig. No.26 :Predicted Medium Energy MsMs Spectrum (20V),  $[M+H]^+$

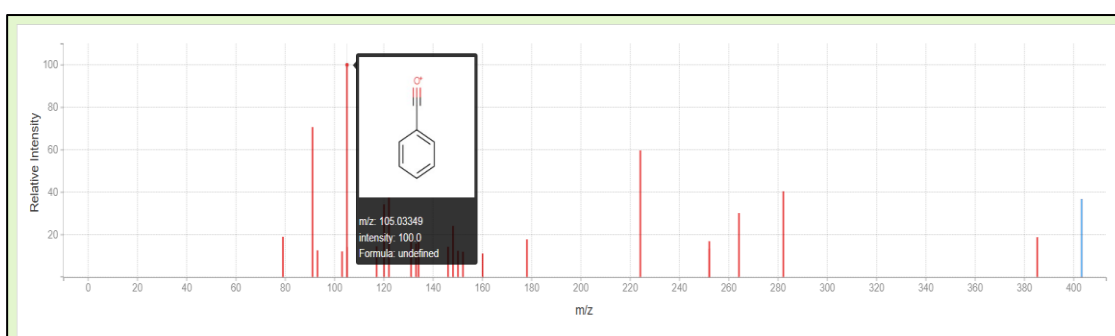


Fig. No.27 :Base peak in Energy (20V),  $[M+H]^+$

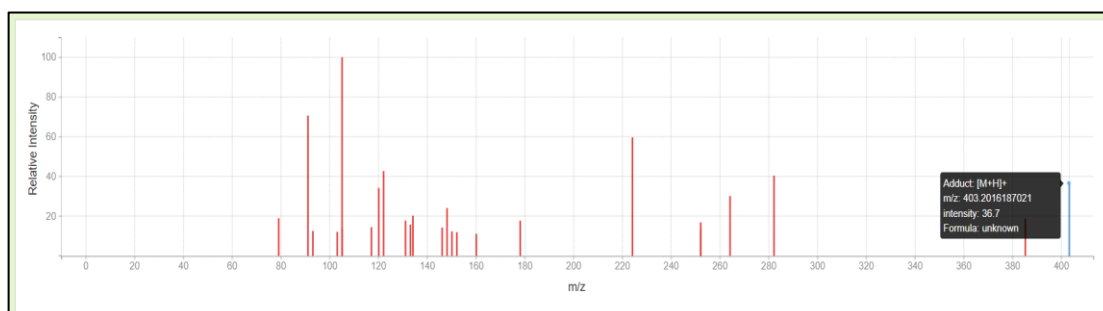


Fig. No.28 :Molecular Ion peak in Energy (20V),  $[M+H]^+$

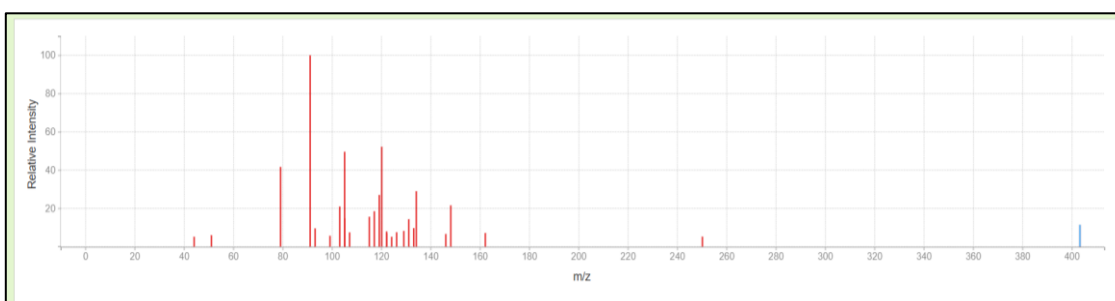


Fig. No.29 : Predicted High Energy MsMs Spectrum (40V),  $[M+H]^+$

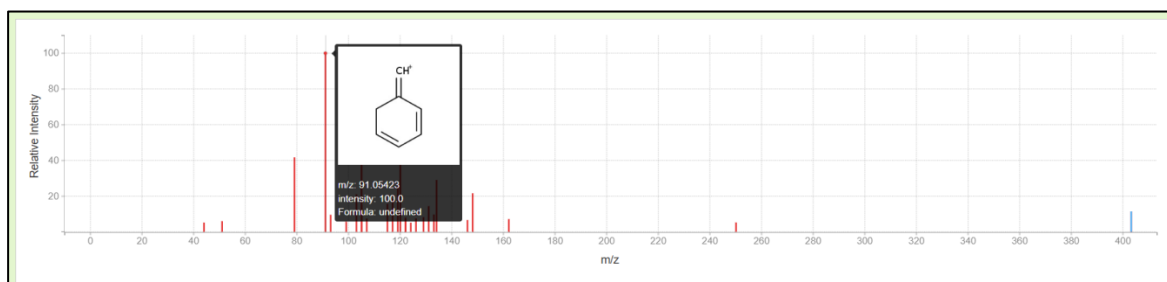


Fig. No. 30 : Base peak in Energy (40V), [M+H]<sup>+</sup>

## NMR SPECTROSCOPY

NMRium webserver predicted the NMR spectra, such as 1D and 2D NMR at the frequency of Frequency 400MHz to elucidate the chemical structure of compound. NMR spectra can easily be loaded by simply dragging and dropping the

corresponding files into the browser. Once the spectra are loaded, NMRium automatically groups them based on their corresponding nucleus. This feature streamlines the data analysis process and enables efficient data interpretation. The 1D and 2D NMR obtained are given below with its ranges

## <sup>1</sup>H- NMR

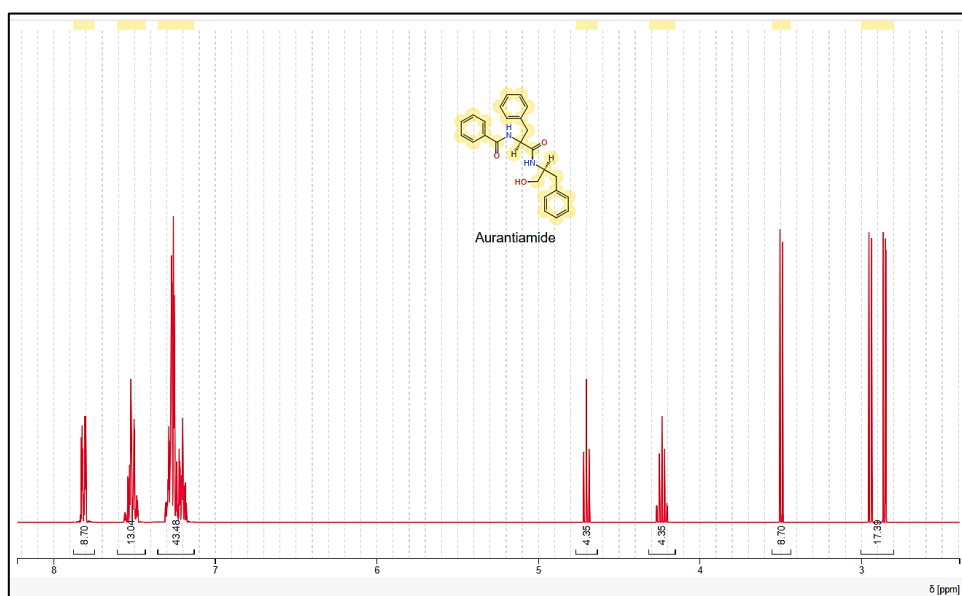


Fig. No. 31 :<sup>1</sup>H NMR spectrum

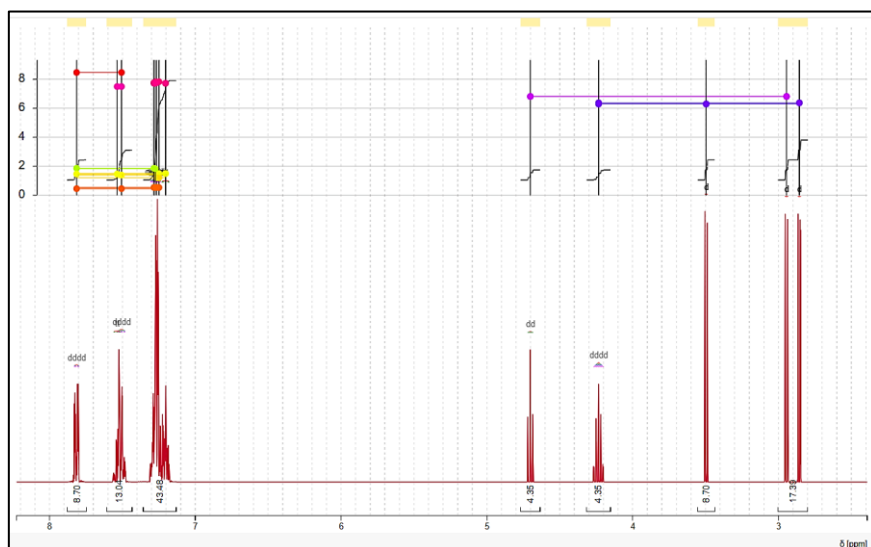


Fig. No. 32 :<sup>1</sup>H NMR spectrum J graph with multiplicity trees

### <sup>1</sup>H NMR Interpretation

<sup>1</sup>H NMR (400 MHz):  $\delta$  2.80-3.00 (4H, 2.86 (d,  $J$  = 6.37 Hz), 2.86 (d,  $J$  = 6.37 Hz), 2.95 (d,  $J$  = 6.81 Hz), 2.95 (d,  $J$  = 6.81 Hz)), 3.44-3.55 (2H, 3.50 (d,  $J$  = 6.29 Hz), 3.50 (d,  $J$  = 6.29 Hz)), 4.23 (1H, dddd,  $J$  = 6.37, 6.37, 6.29, 6.29 Hz), 4.70 (1H, dd,  $J$  = 6.81, 6.81 Hz), 7.13-7.36 (10H, 7.20 (tt,  $J$  = 7.72,

1.49 Hz), 7.20 (tt,  $J$  = 7.73, 1.49 Hz), 7.25 (dddd,  $J$  = 7.83, 1.49, 1.20, 0.53 Hz), 7.26 (dddd,  $J$  = 7.77, 1.49, 1.21, 0.53 Hz), 7.27 (dddd,  $J$  = 7.83, 7.72, 1.83, 0.53 Hz), 7.28 (dddd,  $J$  = 7.77, 7.73, 1.85, 0.53 Hz)), 7.43-7.61 (3H, 7.51 (dddd,  $J$  = 8.47, 7.50, 1.39, 0.45 Hz), 7.54 (tt,  $J$  = 7.50, 1.46 Hz)), 7.81 (2H, dddd,  $J$  = 8.47, 1.86, 1.46, 0.45 Hz).

### <sup>13</sup>C-NMR

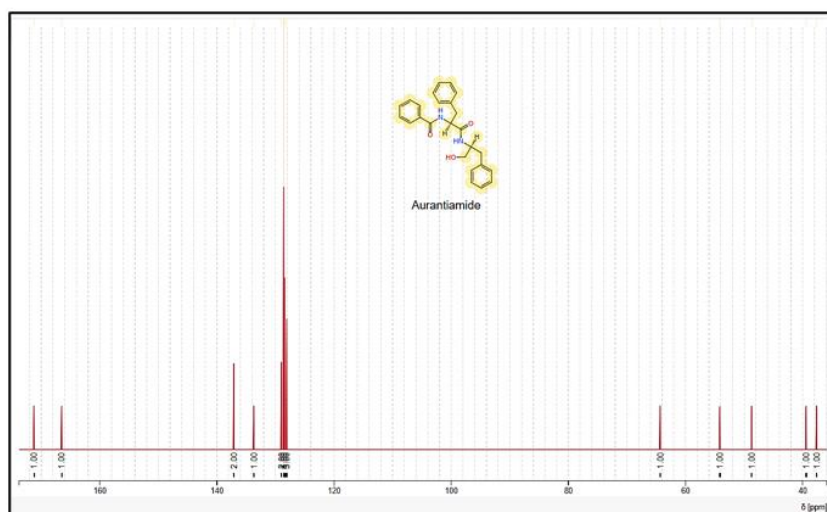


Fig. No. 33 :<sup>13</sup>C NMR spectrum

### <sup>13</sup>C NMR Interpretation

<sup>13</sup>C NMR (101 MHz):  $\delta$  37.60 (1C, s), 39.40 (1C, s), 48.70 (1C, s), 54.13 (1C, s), 64.30 (1C, s), 128.05-128.15 (3C, 128.10 (s), 128.10 (s), 128.10 (s)), 128.35-128.45 (4C, 128.40 (s), 128.40

(s)), 128.55-128.65 (6C, 128.60 (s), 128.60 (s), 128.60 (s)), 129.00 (2C, s), 133.70 (1C, s), 137.06-137.16 (2C, 137.11 (s), 137.11 (s)), 166.50 (1C, s), 171.20 (1C, s).

### $^1\text{H}$ - $^1\text{H}$ (COSY) and $^1\text{H}$ - $^{13}\text{C}$ (HECTOR)

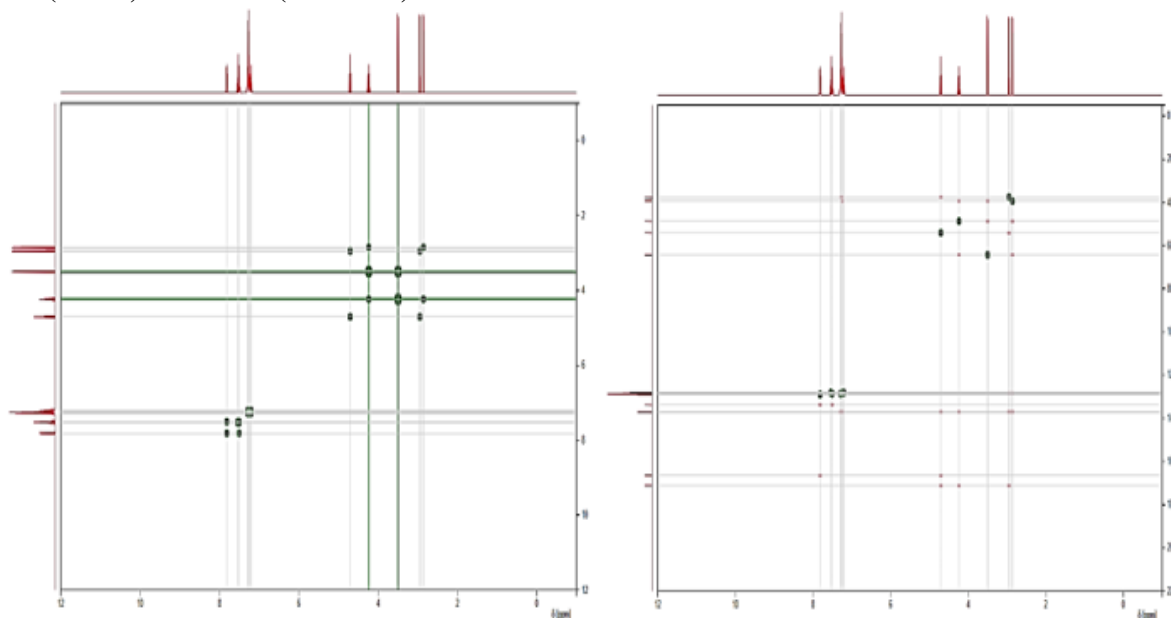


Fig. No. 34 :  $^1\text{H}$ - $^1\text{H}$  and  $^1\text{H}$ - $^{13}\text{C}$  spectrum

## IV. CONCLUSION

From the current research, we found that Aurantiamide is capable of being effective against Multiple sclerosis as an orally bioavailable, non-toxic ligand in drug discovery. Hence, the compound Aurantiamide may be considered as a lead in treatment of Multiple Sclerosis. We also understood that AI-guided drug design fastens the drug discovery process.

## REFERENCE

- [1]. Haki, Maha PhDa; AL-Biati, Haeder A. PhDa; Al-Tameemi, Zahraa Salam PhDa,b; Ali, Inas Sami PhDa; Al-hussaniy, Hany A. PhDa,b,c,\* . Review of multiple sclerosis: Epidemiology, etiology, pathophysiology, and treatment. *Medicine* 103(8):p e37297, February 23, 2024. | DOI: 10.1097/MD.00000000000037297
- [2]. Sabe VT, Ntombela T, Jhamba LA, Maguire GE, Govender T, Naicker T, Kruger HG. Current trends in computer aided drug design and a highlight of drugs discovered via computational techniques: A review. *European Journal of Medicinal Chemistry*. 2021 Nov 15;224:113705.
- [3]. Chang Y, Hawkins BA, Du JJ, Groundwater PW, Hibbs DE, Lai F. A Guide to In Silico Drug Design. *Pharmaceutics*. 2023;15(1):49.
- [4]. Olutola Dosumu O, Onocha P, Ekundayo O, Ali M. Isolation of aurantiamides from *Gomphrena celosioides* C. Mart. *Iran J Pharm Res*. 2014 Winter;13(1):143-7. PMID: 24734065; PMCID: PMC3985246.
- [5]. Chen L, Liu Y, Jia D, Yang J, Zhao J, Chen C, Liu H, Liang X. Pharmacokinetics and Biodistribution of Aurantiamide and Aurantiamide Acetate in Rats after Oral Administration of *Portulaca oleracea* L. Extracts. *J Agric Food Chem*. 2016 May 4;64(17):3445-55. doi: 10.1021/acs.jafc.6b00470. Epub 2016 Apr 21. PMID: 27075043.
- [6]. Fang Z, Fang J, Gao C, Wu Y, Yu W. Aurantiamide Acetate Ameliorates Lung Inflammation in Lipopolysaccharide-Induced Acute Lung Injury in Mice. *Biomed Res Int*. 2022 Aug 22;2022:3510423. doi: 10.1155/2022/3510423. PMID: 36046440; PMCID: PMC9424011.
- [7]. Gallo K, Goede A, Preissner R, Gohlke BO. SuperPred 3.0: drug classification and target prediction—a machine learning approach. *Nucleic Acids Research*. 2022 May 7;

- [8]. Daina A, Michielin O, Zoete V. SwissADME: a Free web Tool to Evaluate pharmacokinetics, drug-likeness, and Medicinal Chemistry Friendliness of Small Molecules. Scientific Reports [Internet]. 2017 Mar 3;7(1). Available from: <https://www.nature.com/articles/srep42717>
- [9]. Osita Sunday Nnyigide, Tochukwu Olunna Nnyigide, Lee SG, Hyun K. Protein Repair and Analysis Server: A Web Server to Repair PDB Structures, Add Missing Heavy Atoms and Hydrogen Atoms, and Assign Secondary Structures by Amide Interactions. Journal of Chemical Information and Modeling. 2022 Aug 24;62(17):4232–46.
- [10]. Laskowski RA, MacArthur MW, Moss DS, Thornton JM. PROCHECK: a program to check the stereochemical quality of protein structures. Journal of Applied Crystallography. 1993 Apr 1;26(2):283–91.
- [11]. Colovos C, Yeates TO. Verification of protein structures: patterns of nonbonded atomic interactions. Protein Sci. 1993 Sep;2(9):1511-9. doi: 10.1002/pro.5560020916. PMID: 8401235; PMCID: PMC2142462.
- [12]. Bowie JU, Lüthy R, Eisenberg D. A method to identify protein sequences that fold into a known three-dimensional structure. Science. 1991 Jul 12;253(5016):164-70. doi: 10.1126/science.1853201. PMID: 1853201.
- [13]. Liu Y, Yang X, Gan J, Chen S, Xiao ZX, Cao Y. CB-Dock2: improved protein–ligand blind docking by integrating cavity detection, docking and homologous template fitting. Nucleic Acids Research. 2022 May 24;
- [14]. Kuriata A, Gierut AM, Oleniecki T, Ciemny M, Kolinski A, Kurcinski M, et al. CABS-flex 2.0: a web server for fast simulations of the flexibility of protein structures. Nucleic Acids Research [Internet]. 2018 May 14 [cited 2020 Mar 13];46(W1):W338–43. Available from: <https://arxiv.org/ftp/arxiv/papers/1802/1802.07568.pdf>
- [15]. Sun H, Cao D, Hou T. fastDRH: a webserver to predict and analyze protein–ligand complexes based on molecular docking and MM/PB(GB)SA computation. Briefings in Bioinformatics. 2022 May 18;23(5).
- [16]. Luc Patiny, Hamed Musallam, Alejandro Bolaños, Michaël Zasso, Julien Wist, Metin Karayilan, Eva Ziegler, Johannes C. Liermann and Nils E. Schlörer. Beilstein J. Org. Chem. 2024, 20, 25-31. <https://doi.org/10.3762/bjoc.20.4>
- [17]. Wang F, Allen D, Tian S, Oler E, Gautam V, Greiner R, Metz TO, and Wishart DS. (2022) CFM-ID 4.0—a web server for accurate MS-based metabolite identification. Nucleic Acids Research 50 (W1), W165-W174.